Inverse Problems Applied to Bolometer Diagnostics in Magnetic Fusion Experiments

Byron Peterson

National Institute for Fusion Science, SOKENDAI

Toki, Japan

with cooperation from:

D. Zhang, IPP; J. Jang, KFE; F. Federici, ORNL

13th ITER International School

December 9, 2024

Outline

- Bolometer diagnostics
  - Bolometry and sources of radiation
  - Resistive bolometers (RB)
  - Imaging bolometers (IRVB)
- Geometry matrix calculation
- Synthetic diagnostics
  - for comparison of plasma model with experimental data
  - utilization for diagnostic design
- Tomography examples:
  - 1D using SVD with RB in LHD
  - 2D using RGS with RB in W-7X
  - 2D using Phillips Tikhonov with 1 IRVB in KSTAR
  - 3D using Tikhonov with 4 IRVBs in LHD
  - 2D using SART and Bayesian with RBs and IRVB in MAST-U
- Conclusion

Bolometry

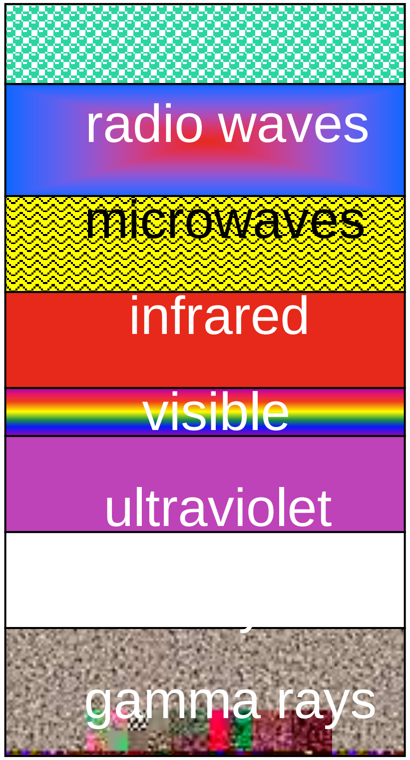
radio waves
microwaves
infrared
visible
ultraviolet
gamma rays

Sources of Radiation

$$(T_e \quad 4 keV, n_e \quad 4 \quad 10^{13}/cm^3, V \quad 30 m^3, Z_{eff} \quad 3, B \quad 2.5 T)$$

free electron - Cyclotron (38 kW)

$$S_c \quad 5 \quad 10^{38} n_e^2 T_e^2 (W/cm^3)$$

ion-electron interaction - Bremsstrahlung (38 kW)

free-bound transition - Recombination

$$S_r \quad 1.7 \quad 10^{32} n_e T_e^{1/2} \quad \underset{Z}{} Z^2 n_Z \frac{E^{Z \quad 1}}{T_e} (W/cm^3)$$

bound electrons - Line radiation of impurities

$$S_{imp} \quad \underset{n,Z}{} n_e n_{n,Z} L_{n,Z}(T_e)$$

Gold Foil Thickness (sensitivity) vs Photon Energy

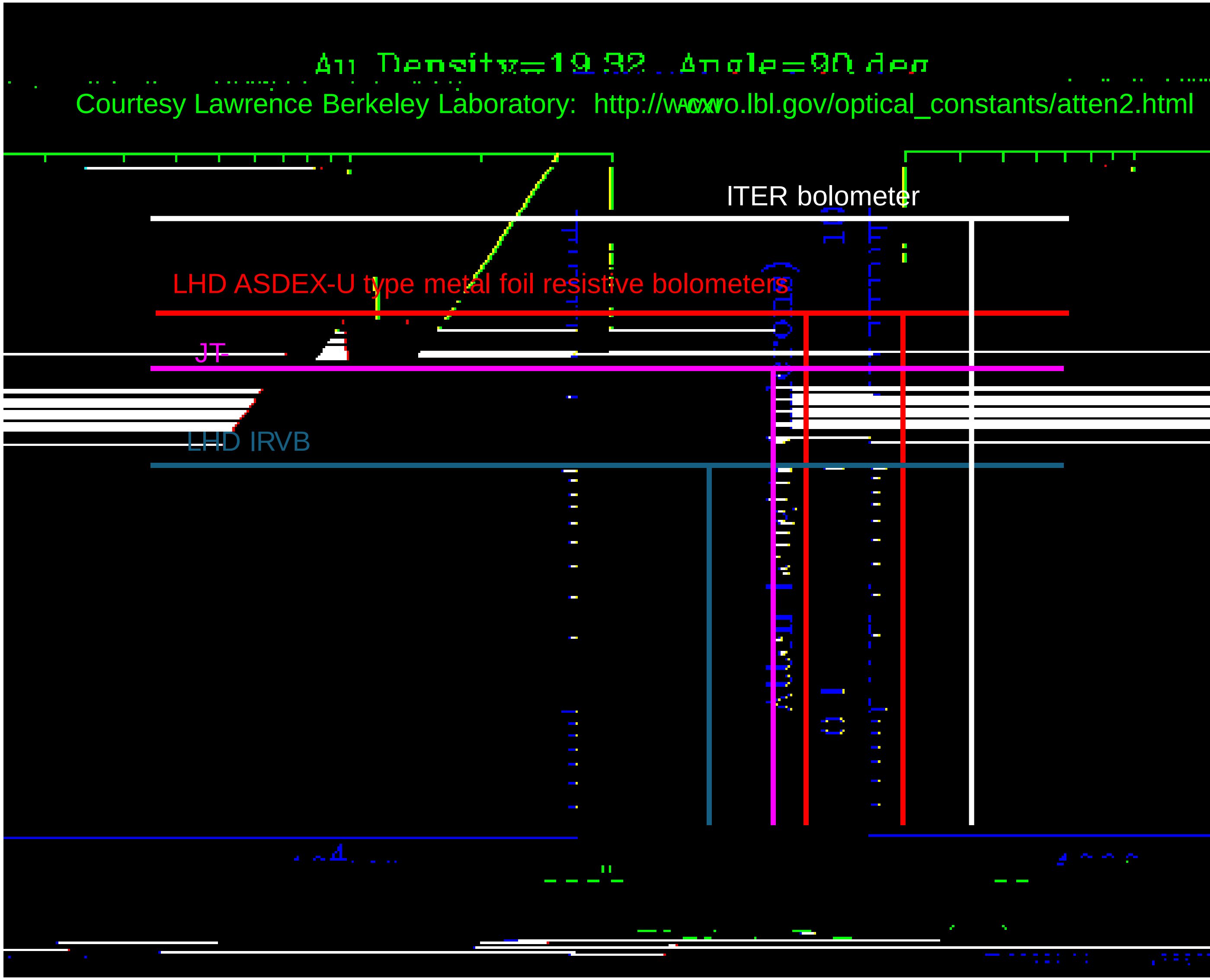

Outline

- Bolometer diagnostics
  - Sources of radiation
  - Resistive bolometers (RB)
  - Imaging bolometers (IRVB)
- Geometry matrix calculation
- Synthetic diagnostics
  - for comparison of plasma model with experimental data
  - utilization for diagnostic design
- Tomography examples:
  - 1D using SVD with RB in LHD
  - 2D using RGS with RB in W-7X
  - 2D using Phillips Tikhonov with 1 IRVB in KSTAR
  - 3D using Tikhonov with 4 IRVBs in LHD
  - 2D using SART and Bayesian with RBs and IRVB in MAST
- Conclusion

Resistive Bolometer Arrays, Calibration and Profile Inversion

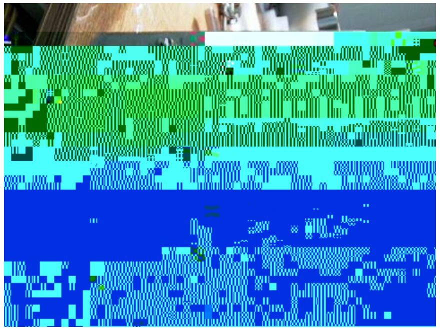

12 channel bolometer array

1D plasma grid definition

assumption: constant on a flux surface

$$P_i \quad {}_j \; \frac{ij}{4} V_{ij} S_j \quad {}_j \; T_{ij} S_j$$

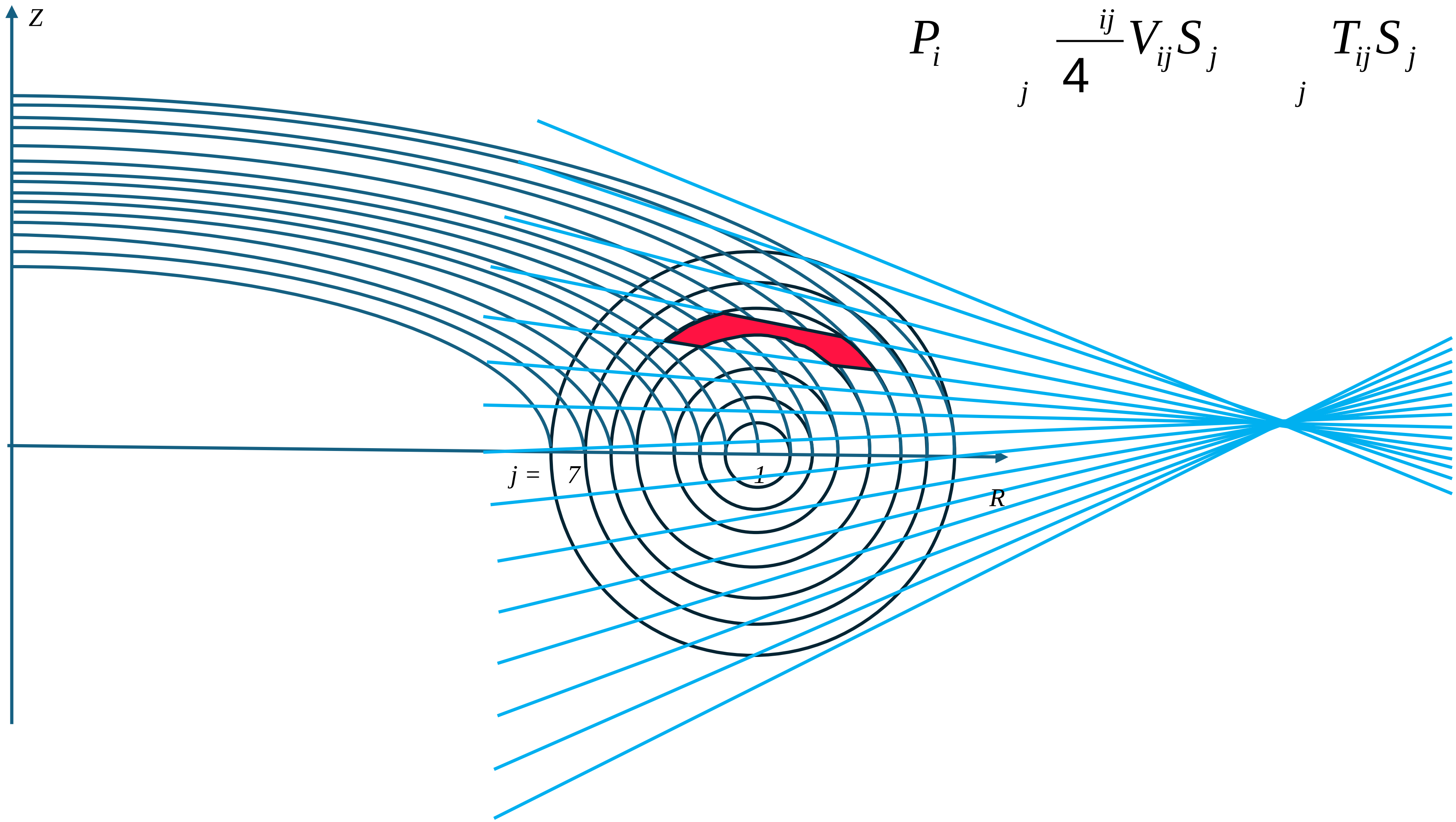

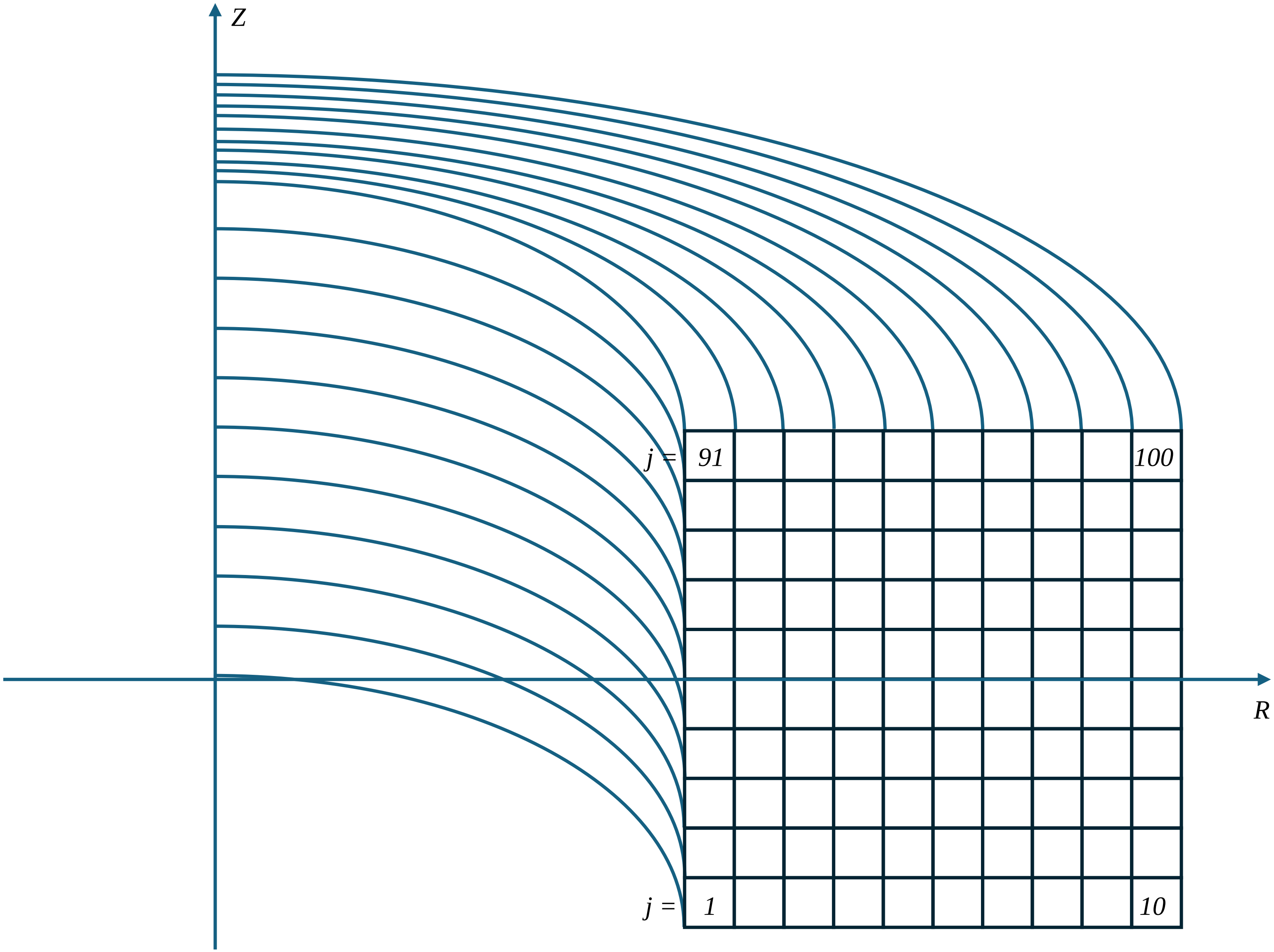

Z
R
j = 91
100
j = 1
10

Resistive Bolometer Arrays, Calibration and Profile Inversion

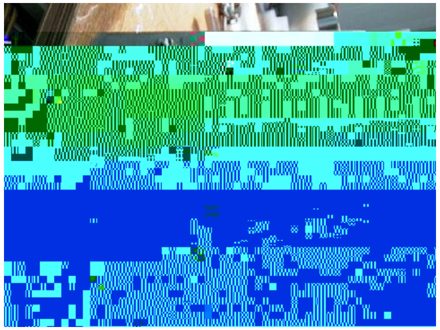

Outline

- Bolometer diagnostics
  - Sources of radiation
  - Resistive bolometers (RB)
  - Imaging bolometers (IRVB)
- Geometry matrix calculation
- Synthetic diagnostics
  - for comparison of plasma model with experimental data
  - utilization for diagnostic design
- Tomography examples:
  - 1D using SVD with RB in LHD
  - 2D using RGS with RB in W7-X
  - 2D using Phillips Tikhonov with 1 IRVB in KSTAR
  - 3D using Tikhonov with 4 IRVBs in LHD
  - 2D using SART and Bayesian with RBs and IRVB in MAST
- Conclusion

Foil temperature from IR camera

Power on foil, P_{rad}

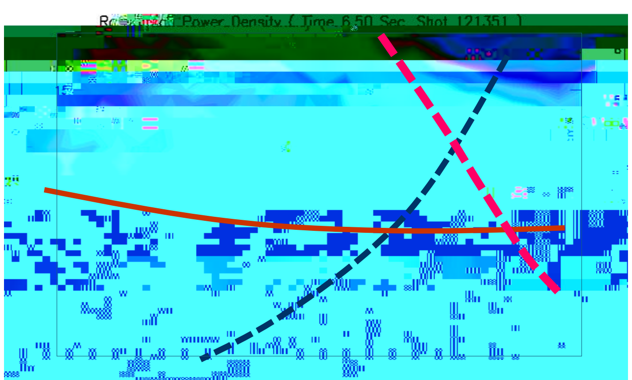

EMC3-EIRENE

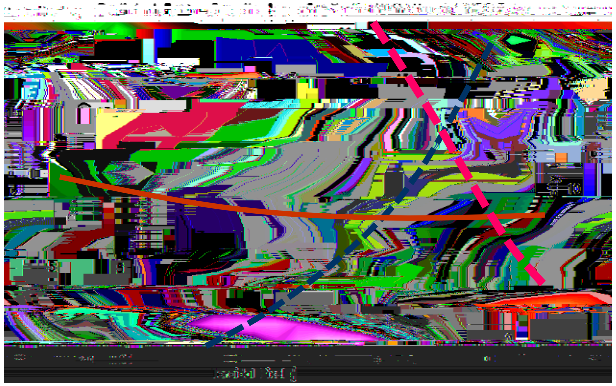

Modeling

Plasma parameters
$n_e(x,t)$, $T_e(x,t)$, etc.

Impurity diffusion coefficients
$D(x,t)$, $v(x,t)$, etc.

EMC3-EIRENE

3D edge carbon radiation estimate

S_j

Field of View

Response matrix T_{ij} $\frac{\ ^{ij}}{4} V_{ij}$

Synthetic image

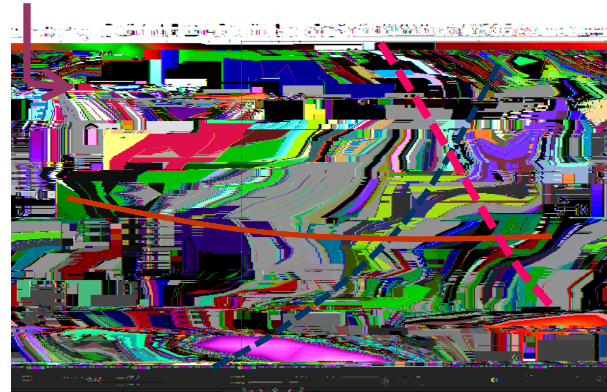

Power at foil, P_{rad}

$P_i \quad \sum_j T_{ij} S_j$

Design of imaging bolometer for ITER using synthetic diagnos

- SANCO provides S( ) in 30 annular regions
- SOLPS provides S(R,Z) in 8866 cells
- Models for the following case are considered:
  - Fuel , 2% Be, 10^{-5} W
- SANCO and SOLPS P_{rad} data resampled:
  - 2 cm R,Z grid 219 (R) x 465 (Z) voxels
- 2 IRVB cases are considered:
  - Tangential view of full cross-section:
    - IR camera 512 x 640, 15 mK, 1000 f/s
    - 15x20 pixels, aperture 6 x 6 mm^2
  - Zoomed view of divertor
    - IR camera 1024 x 1280, 15 mK, 105 f/s
    - 24x32 pixels, aperture 3.75 x 3.75 mm^2
- Projection matrices, H, calculated
  - by 3D integration along sight lines
  - Divided into sub-apertures
  - To keep < 2 cm integration cells
- Synthetic images calculated from:

=å

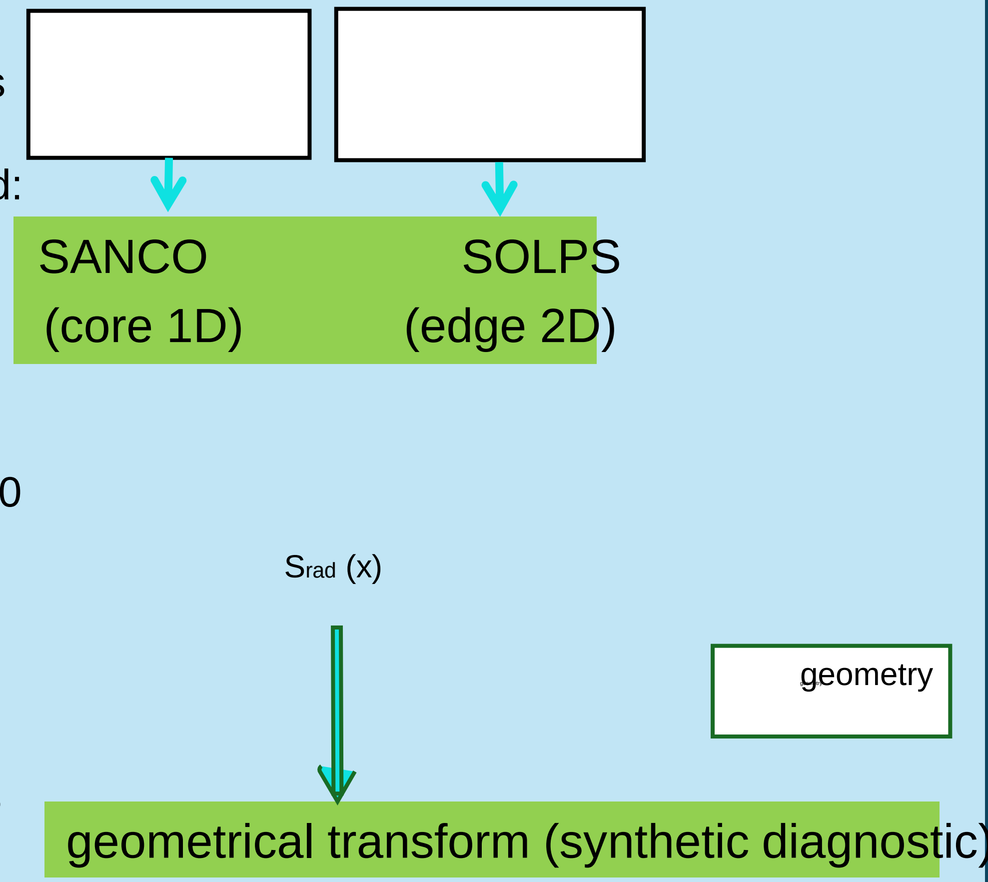

Power spectra shows high energy x-rays from core

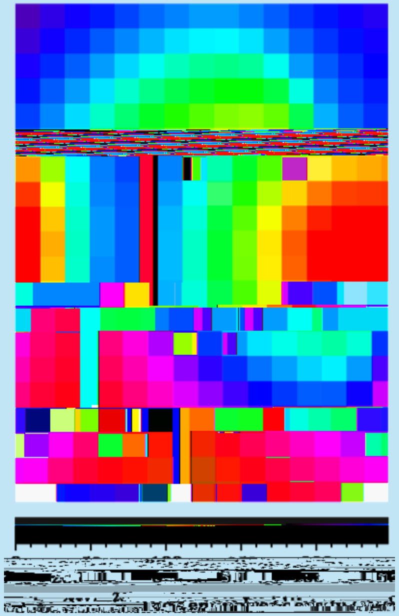

$S_j = S(x,E)$ E

$P_i(E)$

Necessary foil thickness for core IRVB on ITE

$$\frac{}{0}(\quad) = \frac{1}{0} \quad (\quad)\left\{1 - A \right\}$$

Estimation of noise and signal (roughly)

.

~0

[4]

Foil properties (Pt):
k = 0.716 W/cmK foil thermal cond.
= 0.2506 cm^2/s foil thermal diffusivity
t_f foil thickness
A_f = 48 cm^2 utilized area of the foil
IR camera properties:
$_{IR}$ = 15 mK IR camera NET
f_{IR} frame rate of IR camera
N_{IR} number of IR pixels
IRVB properties:
A_{bol} pixel area
f_{bol} frame rate of IRVB
N_{bol} # of bolometer pixels
S_{IRVB} IRVB noise equivalent power density
$_{IRVB}$ IRVB noise equivalent power

Plasma parameters:
L_{plasma} = 10 m length sight line in plasma
P_{rad} = 67.27 MW total radiated power
V_{plasma} = 1049 m^3 plasma volume
Pinhole camera properties:
$A_{ap} = 2.25 * A_{bol}$ area of aperture
$l_{ap\text{-}f}$ distance from foil to aperture
= 10,20 angle between sightline and aperture
S_{signal} estimated radiated power density on foil
$S/N = S_{signal} / S_{IRVB}$ signal to noise ratio

[4] B.J. Peterson *et al., Rev. Sci. Instrum.* **74** (2003) 2040.

$$\frac{\quad}{\quad} \quad \frac{\cos^4}{4 \quad {}^2} \sqrt{\frac{\quad {}^3}{2 \quad {}^3}} \quad \frac{\cos^4}{4 \quad {}^2} \sqrt{\frac{\quad}{2 \quad {}_{bol} \quad {}^3_{bol}}}$$

IRVB	units	Core viewing IRVB		Divertor viewing IRVB	
IR camera parameters					
N_{pix}					
f_{IR}			105		
IRVB parameters					
	m	30		10	
l_{ap-f}	cm	7.8		21.0	
N_{IR}					
N_{bol}					
t_{bol}					
A_{bol}					
A					

Outline

- Bolometer diagnostics
  - Sources of radiation
  - Resistive bolometers (RB)
  - Imaging bolometers (IRVB)
- Geometry matrix calculation
- Synthetic diagnostics
  - for comparison of plasma model with experimental data
  - utilization for diagnostic design
- Tomography examples:
  - 1D using SVD with RB in LHD
  - 2D using RGS with RB in W-7X
  - 2D using Phillips Tikhonov with 1 IRVB in KSTAR
  - 3D using Tikhonov with 4 IRVBs in LHD
  - 2D using SART and Bayesian with RBs and IRVB in MAST
- Conclusion

Resistive Bolometer Arrays, Calibration and Profile Inversion

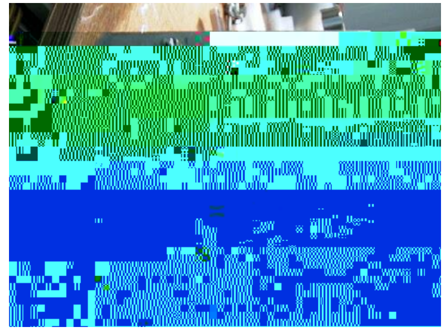

12 channel bolometer array

Detector

Gold foil resistive bolometer

Sensitivity ~ 20 W/cm^2

Blackened with Graphite

Time resolution 10 ms

56 channels installed in LHD

Calibration

$$P_{rad} \quad \frac{1}{K} \quad V_b \quad \frac{V_b}{t}$$

Profile Inversion

CAD drawing of bolometer sight lines and magnetic surfaces

Singular Value Decomposition

'SVD is also the method of choice for solving most linear least squares problems' – W.Press et al. in *Numerical Recipes*

$$\begin{pmatrix} P_1 \\ . \\ . \\ . \\ P_M \end{pmatrix} \quad \begin{pmatrix} T_{1,1} & T_{\dots,1} & T_{N,1} \\ . & \dots & . \\ T_{1,.} & \dots & . \\ . & \dots & . \\ T_{1,M} & \dots & T_{N,M} \end{pmatrix} \quad \begin{pmatrix} S_1 & \dots & S_N \end{pmatrix}$$

$$_{M} \quad ^{N}{}_{N\ M} \quad _{M} \quad ^{N}{}_{N\ M} \quad w \quad w_N \quad V \quad V_N \quad V \quad V_{\ N} \quad V_{N\ N} \quad ^{T}$$

P – power of M detectors

S – power density of N volumes

T – M x N geometry matrix

U – M x N column orthonormal matrix

V –

1D tomographic inversion - sample data

$P_i \left(\ W\right)$

channel number i

$S_j\ (kW/m^2)$

$$P_i \quad {}_j \ \frac{{}_{ij}}{4} V_{ij} S_j \quad {}_j \ T_{ij} S_j$$

j

$$P_i \qquad {}_{j} \; \frac{ij}{4} V_{ij} S_j \qquad {}_{j} \; T_{ij} S_j$$

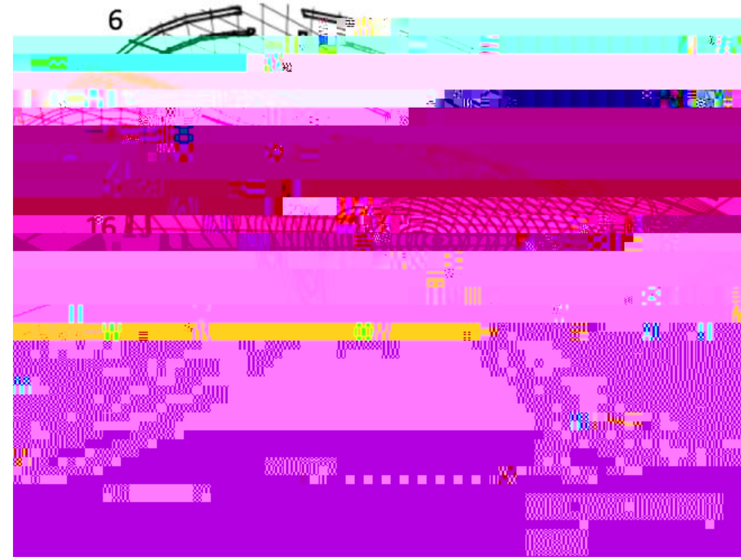

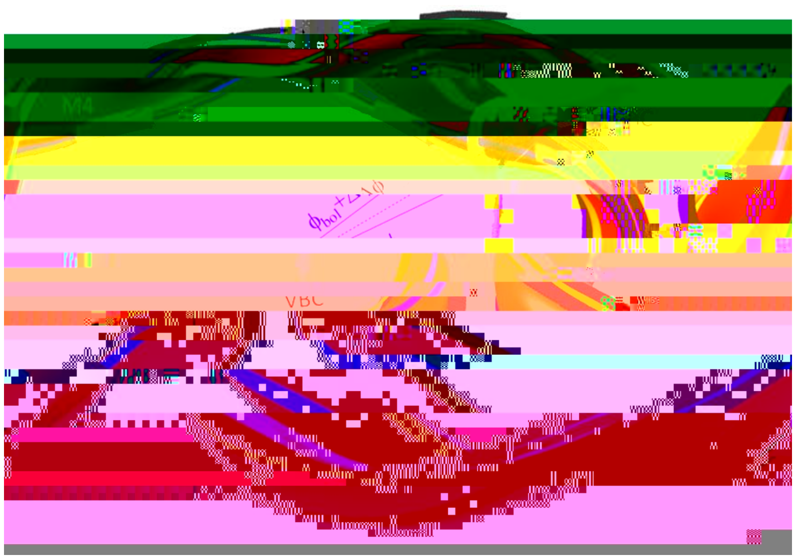

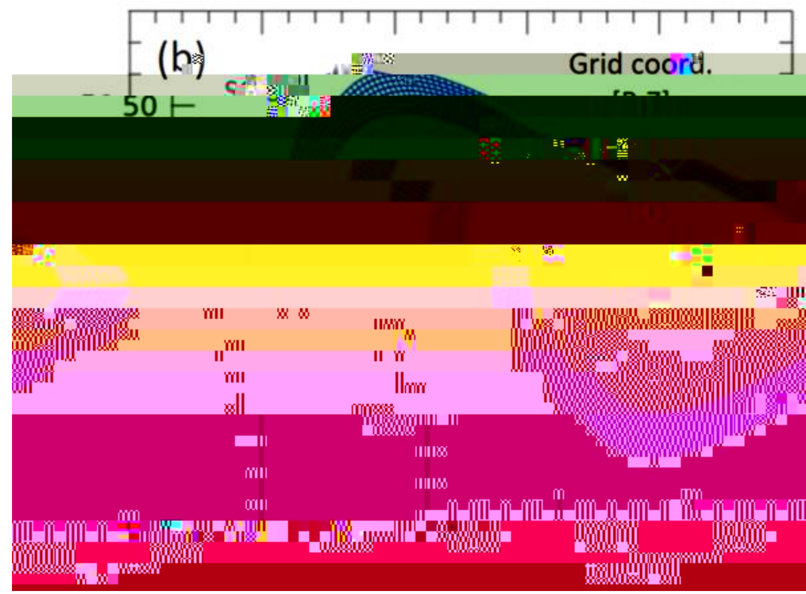

Geometry matrix calculation in W7-X

$$= \left[\frac{\cos(\alpha)\cos(\ \ )\quad A_S}{4\quad{}^2}\right] \quad , \qquad = 1, \ldots, \quad - 1$$

$$= \sigma_{=1} \qquad ,$$

i

The challenges:

unknown parameters >> known conditions

!

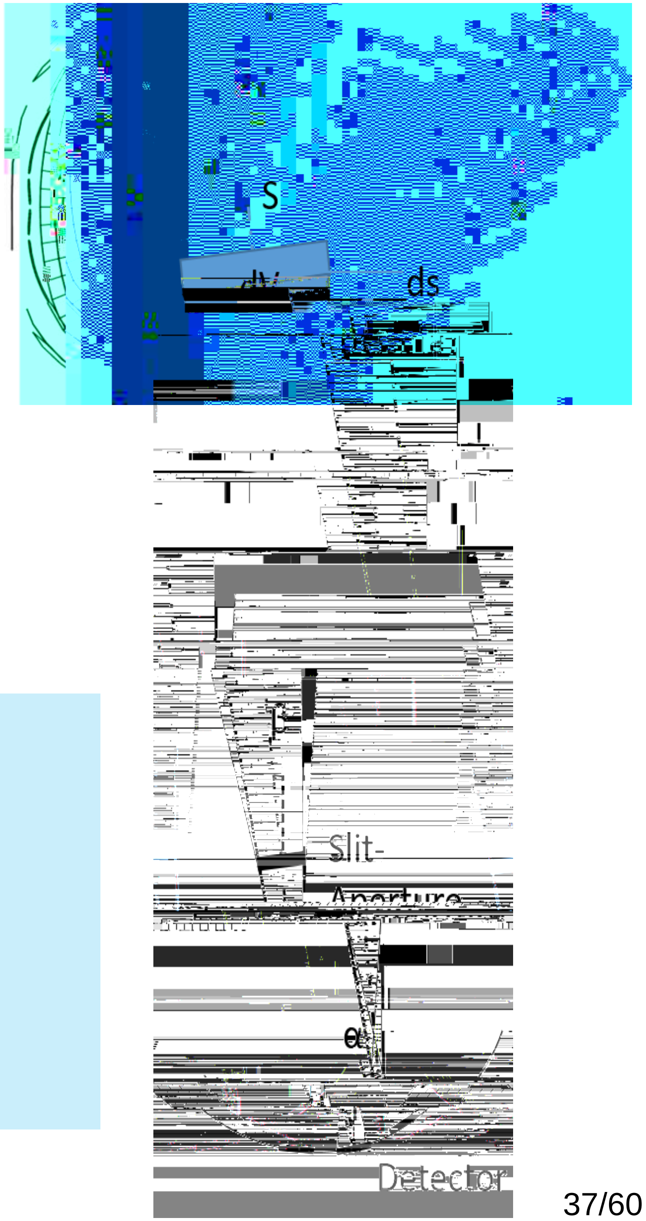

A novel regularization functional invoking anisotropy: relative gradient smoothing (RGS)

Wen

Imaging Bolometer for ITER: Advantage of Toroidal View

Top view of ITER mid-plane

Lower toroidal arr5y

Toroidal arr5y

Semi-toroidal arr5y

Poloidal arr5y

As arrays become more toroidal spatial and angular cover5/ improve

Poloidal projection of LOS:

Maps lines of sight (LOS) back to one poloidal cross-section to show spatial cover5ge assuming axi-symmetry

analysis tools developed by L.C. Ingesson

Imaging Bolometer for ITER: Advantage of Toroidal View

Top view of ITER mid-plane

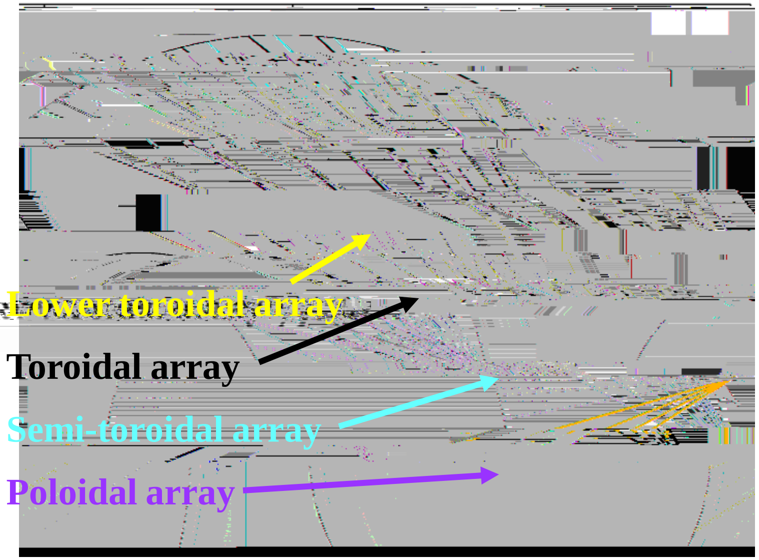

As arrays become more toroidal spatial and angular coverage improve

analysis tools developed by L.C. Ingesson

Poloidal projection of LOS:

Maps lines of sight (LOS) back to one poloidal cross-section to show spatial coverage assuming axi-symmetry

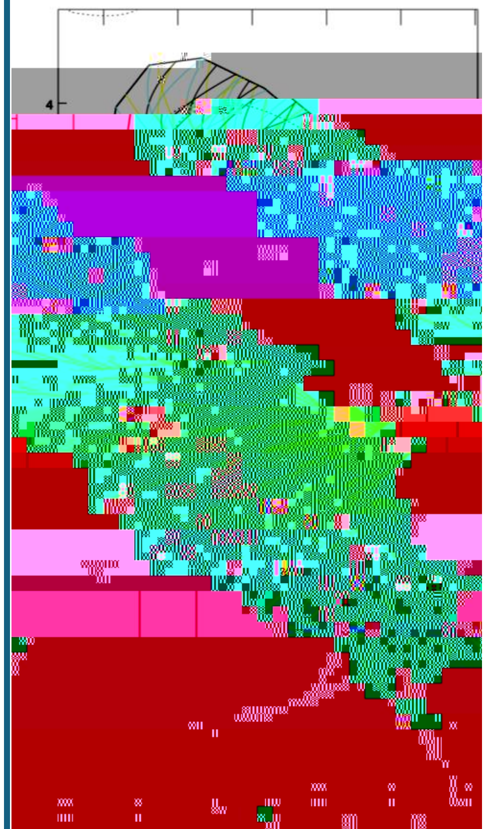

Compared with multiple resistive bolometer camera arrays at one poloidal cross-section

KSTAR IRVB with tangential view

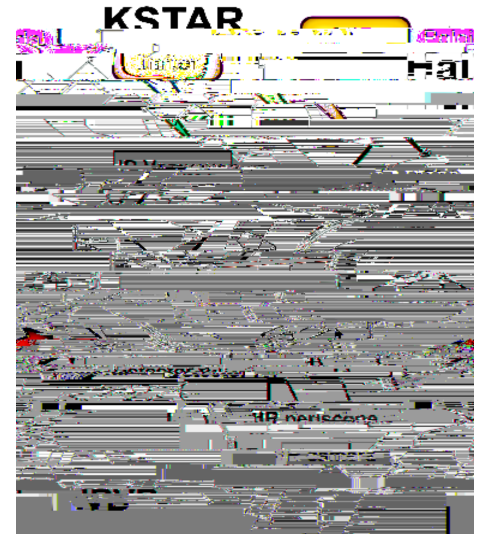

Platinum foil

Size : 0.002 x 70 x 90 mm

Double side carbon coating

IRVB system

Time resolution : 10 ms

24(tor) x 32 (pol) = 384 ch

IR camera : FLIR SC7600

Detector : InSb (Indium Antimonide)

NETD : < 20mK

Spectral range : 1.5 ~ 5.1 um

Frame rate : 105 Hz

Resolution : 512 x 640 pixels

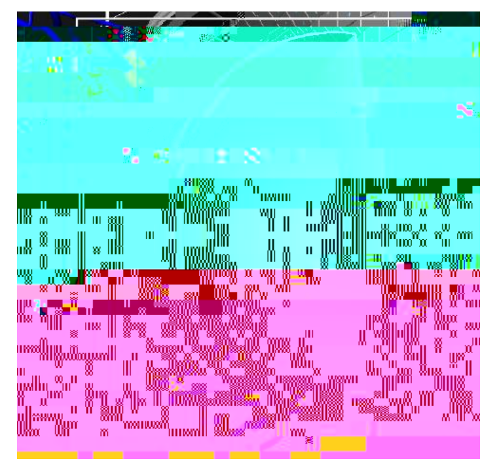

IRVB field of view

Phillips

Reconstruction grid

2 cm x 2 cm pixel was used for reconstruction test

Reconstruction for pixels smaller than 1cm is ongoing for P_{SOL} calculation.

Material boundary condition of KSTAR is applied to reconstruction code.

12x16 → 24x32 channels

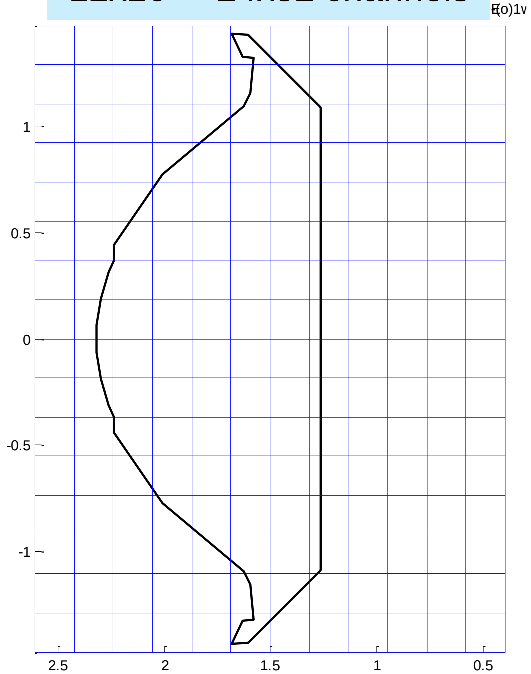

Bolometer view

1.27 < R < 2.52m,
-1.5 < Z < 1.5m

63x150 pixels
(~2x2 cm^2/pixel)

Reconstruction grid

No emission on boundary
$\varepsilon_b = 0$

Region between Passive Stabilizers (-0.5m < Z < 0.5m)
$\varepsilon_b \neq 0$

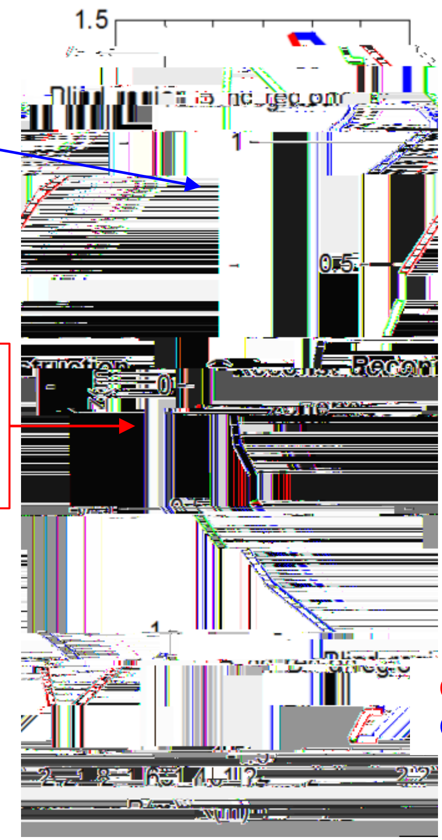

Open
Closed

Boundary condition of divertor

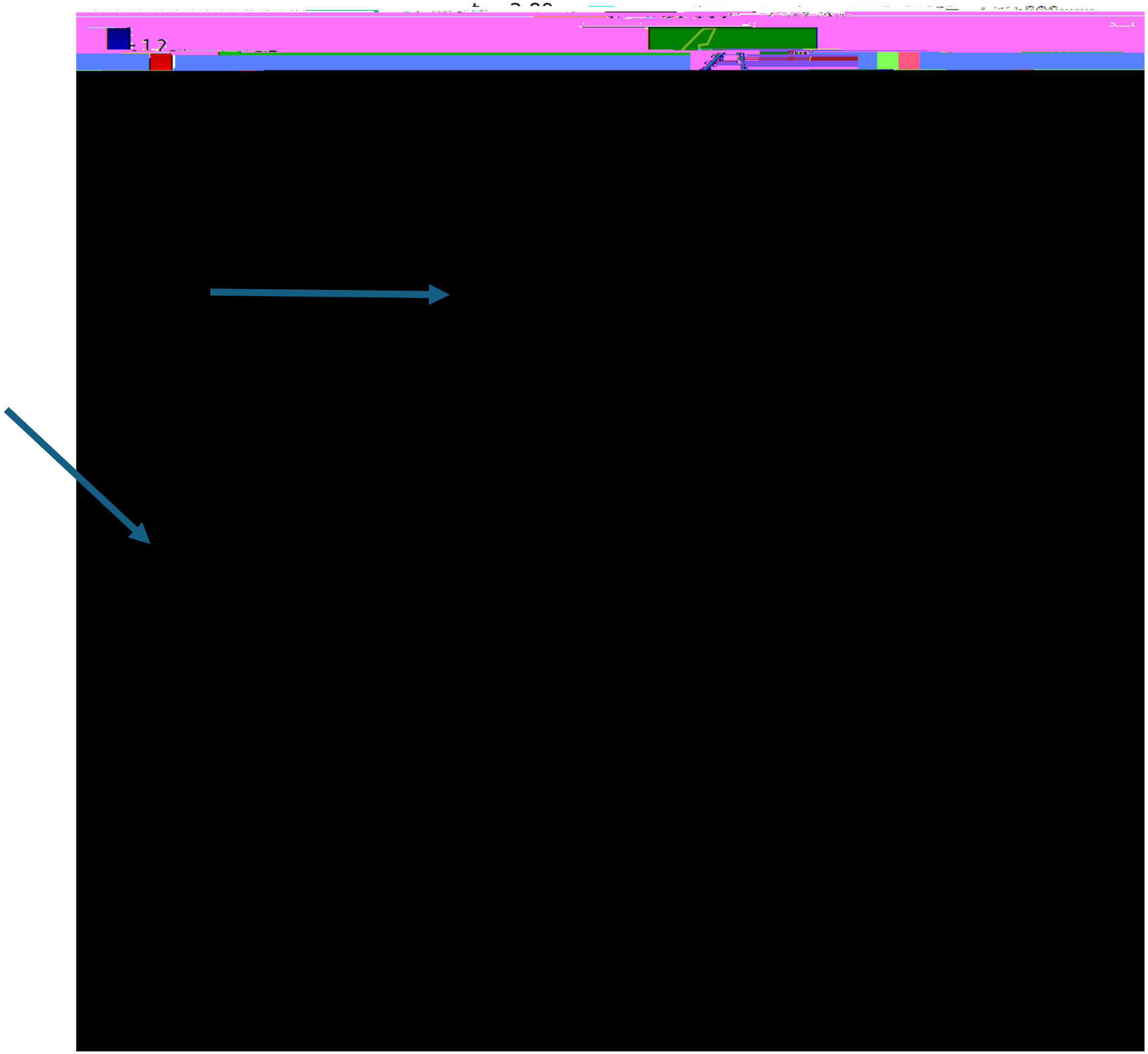

Plasma is divided into volumes using R, z,

R cm, z = 5 cm, = 1 degree

2.5 m < R < 5.0 m (50 divisions)

-1.3 m < z < 1.3 m (52 divisions)

= 0 - 18 degrees (18 divisions) assume helical symmetry

total 46,800 cells

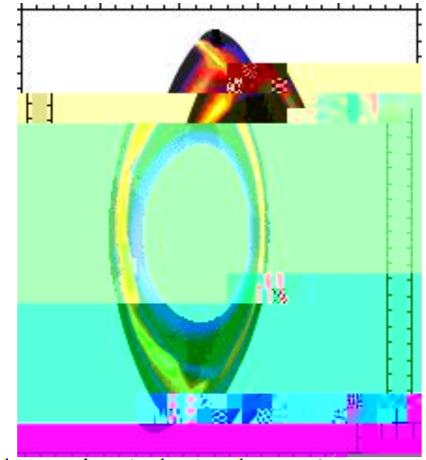

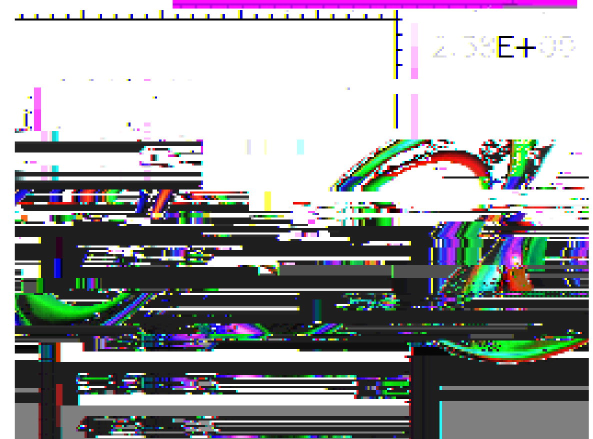

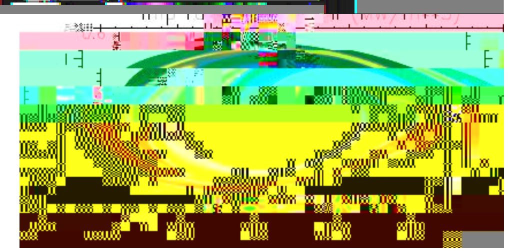

3D radiation profile related to IRVB images by geometry matr

H:Projection matrix (Field of

$$\mathbf{P} = \mathrm{H}\boldsymbol{S}$$

Tikhonov regularization for 3D plasma reconstructi

H: Geometry matrix

P: IRVB data

S:3D radiation profile

M: IRVB channel number

: Regularization parameter

I: Identity matrix

$$\hat{S} = \sum^{M} w_j a_j I^{-1} \mathbf{v}_j$$

$$w_j = \frac{1}{\cdots}$$

$$\langle \mathbf{u}_j \cdot \mathbf{P} \rangle$$

[2]N. Iwama *et al*., J. Plasma Fusion Res. **82** (7), 399 (2006)

3D tomographic inversion shows radiation region shrinks from inboard to outboard.

LHD #121787 Rax=3.9m

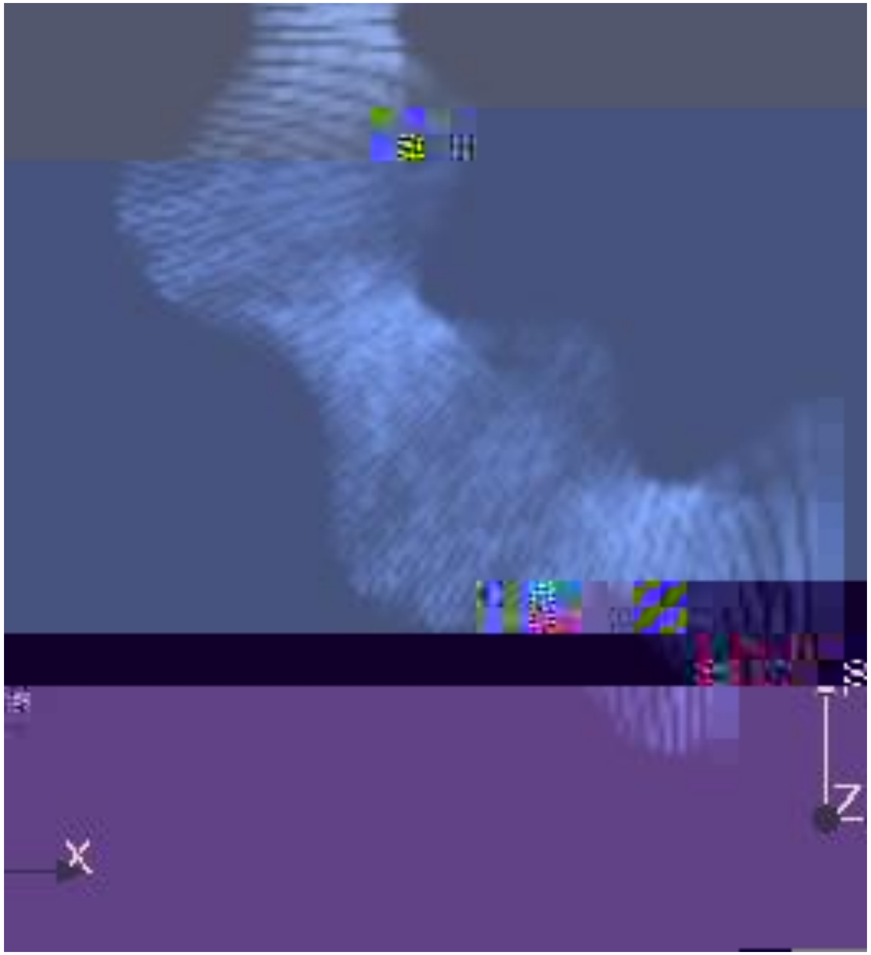

-
-

Once the geometry and area of the foil is defined a method to perform the inversion can actually be devised

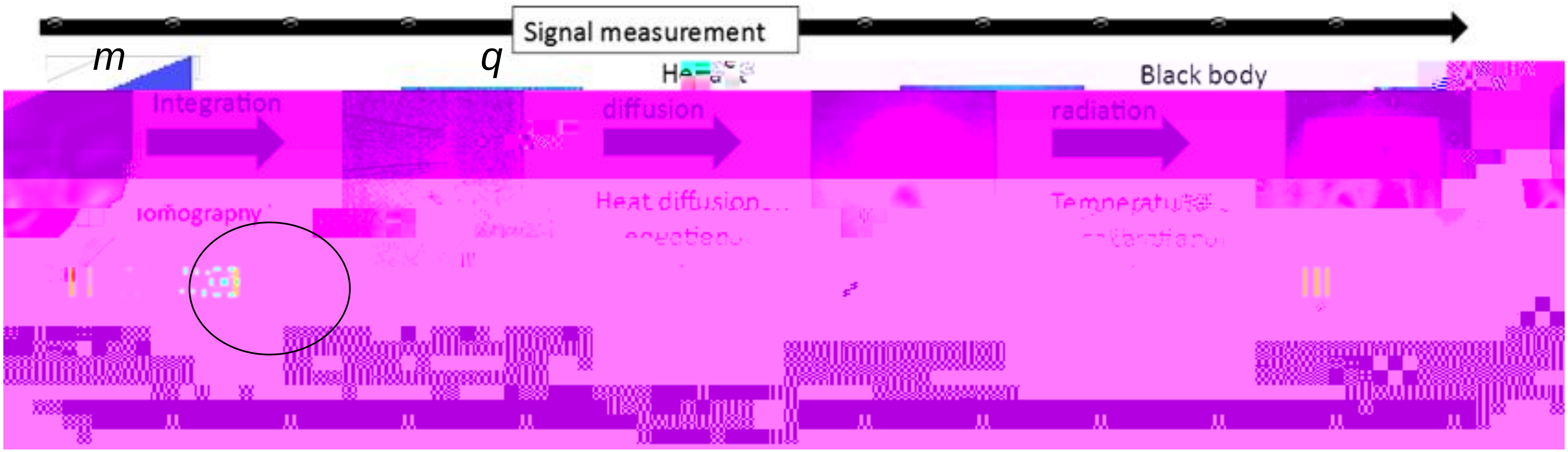

Ideally:

$$\|\mathbf{W}m - q\| = 0$$

with

W = geometry matrix

r = residuals

m = real emissivity solution

q = theoretical brightness measurement

With real data solving for *q* would return an exact solution, but dominated by noise

SART with Phillips-Tikhonov Regularization

- Simultaneous Algebraic Reconstruction Technique (SART)
  - Iterative technique to find solution *m'*
- penalty function ***L***
  - weight given to each spatial pixel in relation to each other and
- regularization coefficient α
  - introduced to limit the irregularity of the solution:

- This is ≠ 0 and it is minimized to find the solution.
- Different types of penalty functions depending on what type of

Bayesian approach considers other factors

Bayesian approach:

Signal noise: The measured camera data is evaluated based on its uncertainty (σ_k).

$$||\mathbf{W}m' - q||$$

$$1 \sum^{m} \left(q_k - \hat{q}_k \right)^2$$

Further corrections:

Contribution to foil brightness due to the pinhole plate heating

Black body radiation due to the pinhole plate heating modelled based on Tmin, Tmax, and the slope of the temperature curve

Aperture plate heated by the plasma radiation and reradiates heating foil

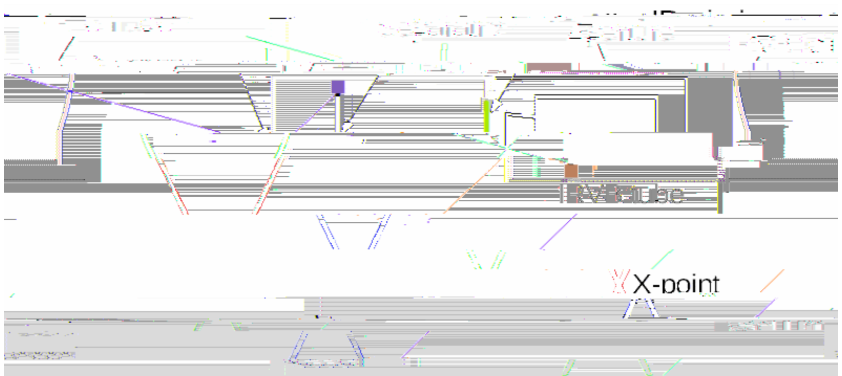

Tmin

Comparison using self-generated phantom

T-P SART

Phantom

Bayesian

Non field aligned feature, unphysical

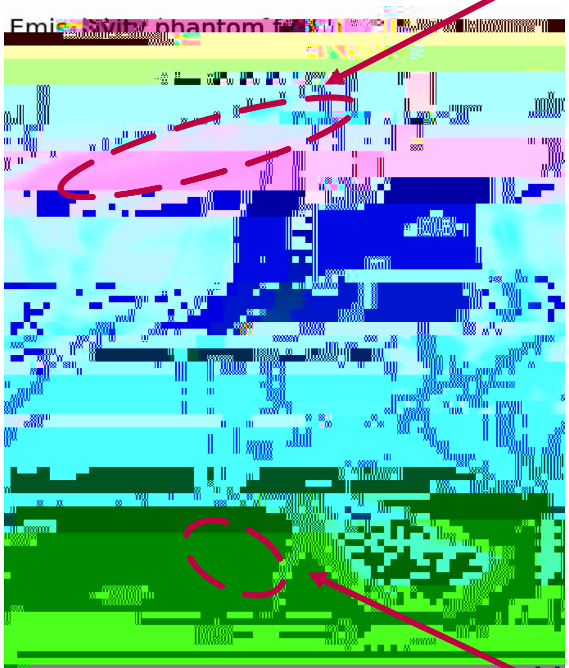

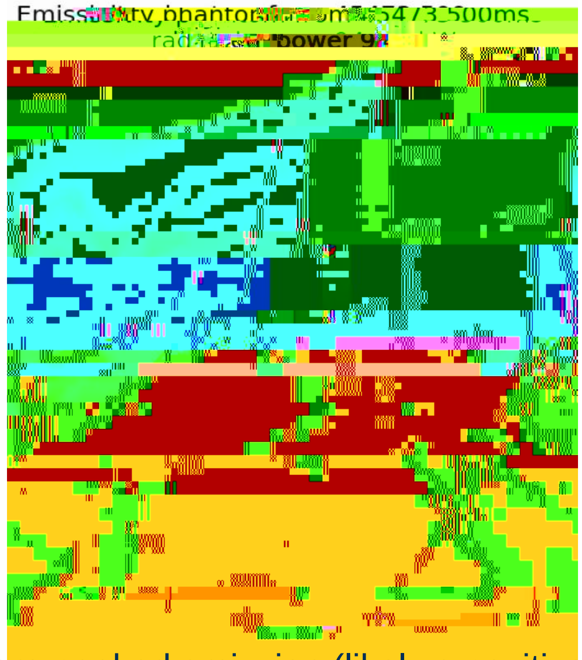

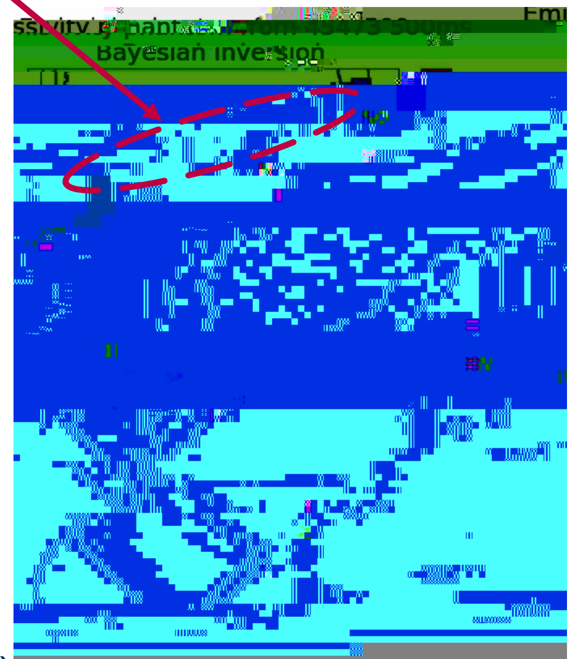

More peaked emission (likely a positive)

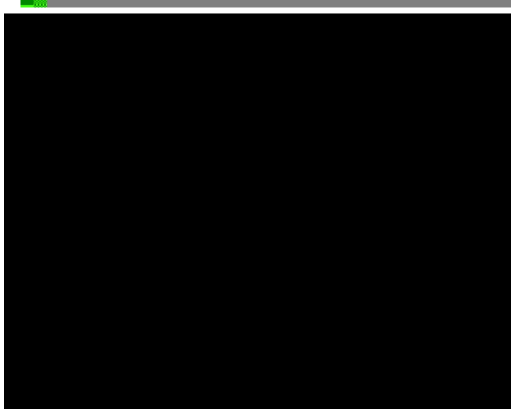

Comparison between SART/Bayes results and the input phantom	SART	BAYES
Radiation std all volume [W/m^3]	675.7	

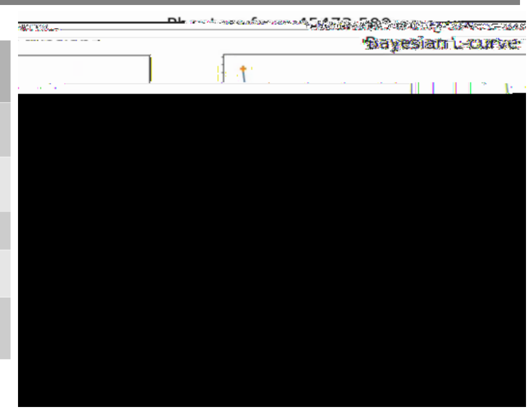

Comparison using real data

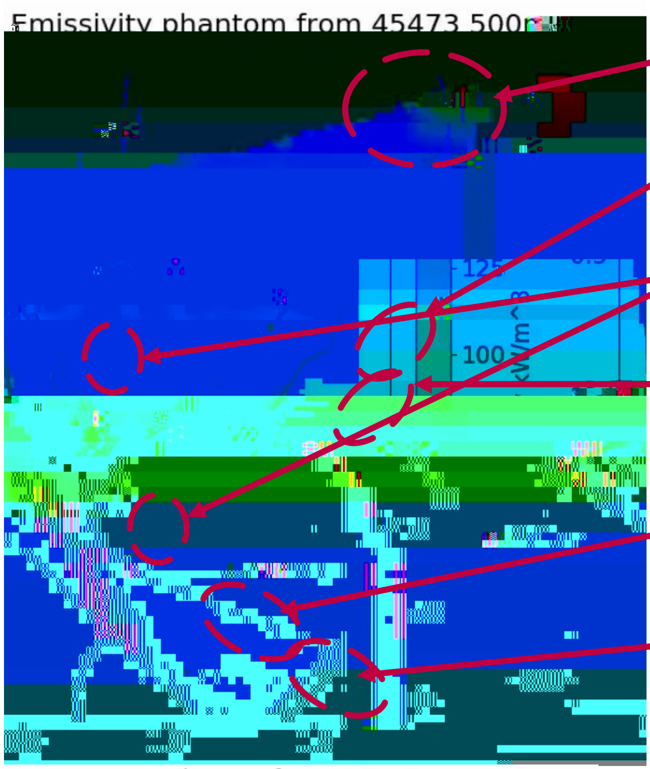

Non field aligned artifacts, unphysical

High emissivity stripes aligned to the pinhole LOS

High emissivity close to surfaces far from separatrix, unphysical

Strong brightness as close as possible to the pinhole (compensates for offsetts)

More peaked emission (likely a positive)

Radiated power elongated in the super-x chamber

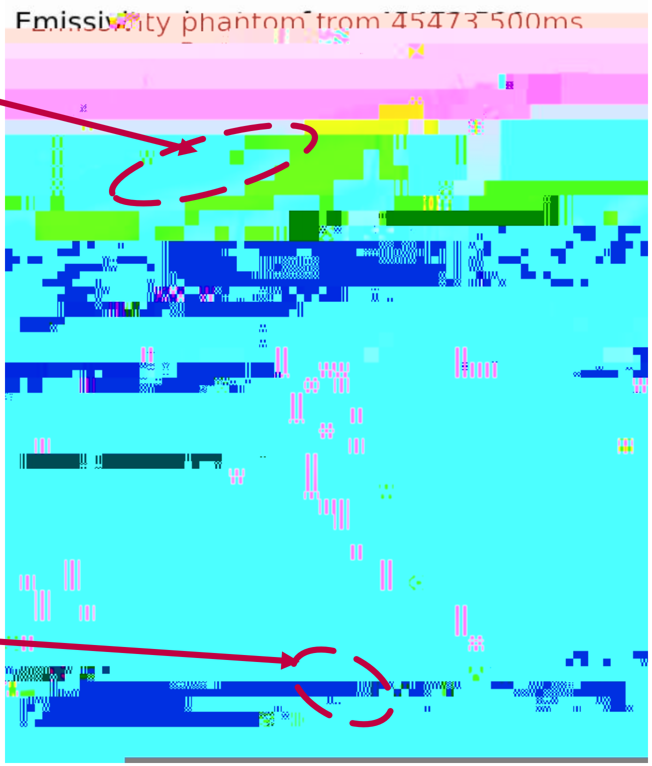

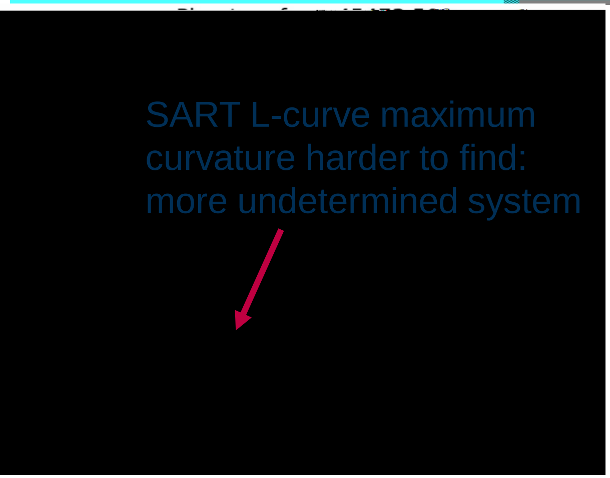

Conclusions

- Bolometers measure total radiated power from plasma
  - Resistive bolometers used in 1D arrays for 1D or 2D tomography at one toroidal angle
  - Imaging bolometers can provide thousands of channels
    - with a 2D (toroidal and poloidal) view of plasma
    - In a tokamak (axisymmetry) with tangential view enables 2D tomography
- Geometry matrix links local and FoV integrated information and used for:
  - Synthetic instrument
    - Direct comparison with line-integrated data
    - Diagnostic design
  - Tomography
- Tomography
  - Used for converting line-integrated data to local information in 1, 2, 3D
    - you define the plasma grid depending on assumptions and detector type and numb
  - Regularization is used in under-determined problems to make trade off between information and stability
  - Different schemes can be used to consider:
    - Anisotropy in radiation profiles with poloidal asymmetry (RGS in a stellarator)
    - Spurious signals, other diagnostics, detector noise, negative values, etc. (Bayesia

Conclusions

- Bolometers measure total radiated power from plasma
    - Resistive bolometers used in 1D arrays for 1D or 2D tomography at one toroidal angle
    - Imaging bolometers can provide thousands of channels
        - with a 2D (toroidal and poloidal) view of plasma
        - In a tokamak (axisymmetry) with tangential view gives 2D tomography
-